DECONVOLUTION OF SPARSE SPIKE TRAINS ACCOUNTING FOR WAVELET PHASE SHIFTS AND COLORED NOISE

F. Champagnat, J. Idier and G. Demoment

Laboratoire des Signaux et Systèmes
École Supérieure d'Électricité
Plateau de Moulon, 91192 Gif-sur-Yvette Cedex, France

ABSTRACT

In this communication we adress the problem of the restoration of spiky sequences when the usual convolution model is corrupted by nonstationnary wavelet phase-shifts. To this end, we introduce an extended convolution model driven by a Bernoulli-Gaussian (BG) like process. This new setting lends itself to easy extension of algorithms designed for BG deconvolution. A comparison of practical results obtained with this new method and BG deconvolution is provided.

1 INTRODUCTION

The subject of this communication is the restoration of spiky sequences distorted by a linear system and an additive noise. Such a problem arises in areas such as seismic exploration, non destructive evaluation (NDE) and biomedical engineering (BME). A widely used model for observed time series (*e.g.* seismic traces, echograms ...) is a convolution of the wavelet, *i.e.*, the incident waveshape and the reflectivity or logarithmic derivative of the impedance which characterizes the unknown medium, plus output noise [1]-[4]. The problem is to restore the reflectivity from observations, given some information on the wavelet and on the noise.

The ill-posedness of deconvolution can be coped using a Bayesian approach. In the case of a stratified media with homogeneous layers, the reflectivity may reasonnably be described *a priori* as a sparse spike train. Mendel and coworkers [1] [2], followed by others [3], proposed a Bernoulli-Gaussian (BG) description for such inputs. Derived estimators and algorithms lead to satisfactory results at a rather modest computational cost when the data is in agreement with the underlying hypothesis, but they are very sensitive to model mismatches, especially to time-varying wavelets. In many practical cases, at least in NDE and BME, the spectral content of the wavelet may be considered almost constant on a sufficiently short time window. On the other hand, significant phase shifts may occur between contiguous reflections. This is evidenced by the spurious reflectors ("false alarms") added by BG-type algorithms, even for slight phase shifts. The same behaviour is experienced in presence of organized noise which may be mistaken for a reflecting event.

The authors wish to thank Électricité de France (REME dept.) for providing the real data presented in this paper.

The main contribution of this paper is to describe the observations in term of a new input-output (I/O) model, driven by a BG-like process, the "Double BG" (DBG) process, accounting for possible phase shifts distorting the wavelet (Section 2). In this new description, each potential reflector is assigned a complex number (compared to a real number in the BG case), whose phase angle represents a phase shift of the wavelet, whereas its modulus represents a scaling factor on the shifted wavelet. Then, in section 3, we fully exploit the MA representation of the wavelet introduced in [3] to yield straightforward extensions of existing methods and algorithms for BG models.

The second contribution is the incorporation of a colored noise model together with the DBG model, in order to fit real data closer. Special attention is paid to careful parameterization and computational efficiency. The conjunction of the two extensions leads to a computational load about eight times larger than its white-noise BG counterpart. On the other hand, the robustness of restoration for real data is improved drastically. Examples of both synthetic and real data processing are provided in section 4.

2 DOUBLE BG MODELING AND RESTORATION

The usual I/O convolution model assumes a time-invariant wavelet $h(.)$:

$$z(k) = \sum_{i=0}^{l} h(i)r(k-i) + n(k), \; k = 1..M, \qquad (1)$$

where z, r and n denote the observations, the unknown reflectivity and observation noise respectively. In this model, the observations consist of the degraded sum of time-shifted wavelets, each of which being scaled by the local value of the reflectivity. In the new proposed

0-7803-0946-4/93 $3.00 © 1993 IEEE

model, not only the scale of the wavelet is altered, but also the phase. The assumed phase shift derives from the area of seismic exploration [4]: let zero phase shift stands for the original wavelet $h(.)$ and $\pi/2$ for its Hilbert transform $g(.)$. Any other phase-shifted wavelet $h_\phi(.)$ is defined by: $h_\phi(.) \triangleq \cos\phi\, h(.)+\sin\phi\, g(.)$. Then the previous I/O model (2) must be replaced by the following one:

$$z(k) = \sum_{i=0}^{l} h(i)r(k-i) + \sum_{i=0}^{l} g(i)s(k-i) + n(k), \quad (2)$$

where r and s can be thought as the real and imaginary part of a unique complex reflectivity function. Thus, we keep a linear I/O structure with a real bivariate (*i.e.* a complex) input and a real scalar output. Equation (2) may be cast in matrix form:

$$\mathbf{z} = H\mathbf{x} + \mathbf{n},\ H = \begin{bmatrix} H_1 & H_2 \end{bmatrix} \text{ and } \mathbf{x} = \begin{bmatrix} \mathbf{r} \\ \mathbf{s} \end{bmatrix}. \quad (3)$$

H_1 and H_2 are $(M \times N)$-matrices and N typically depends on windowing assumptions on the input. The noise $\mathbf{n}$ is assumed Gaussian, centered, of known covariance Γ_n, and independent of $\mathbf{x}$. Recovering $\mathbf{x}$ from the data $\mathbf{z}$ and the matrices H and Γ_n is a new ill-posed problem which will still be treated in a BG Bayesian framework: since the complex reflectivity sequence is also assumed to be sparse, we introduce a "Double BG" process as the input model. The latter can be expressed as a white process (q, r, s):

- $q(k)$ is a Bernoulli variable, with $\lambda \triangleq P(q(k) = 1)$.
- Given $q(k)$, $(r(k), s(k))$ is a zero-mean Gaussian vector with covariance $r_x q(k) I_2$.

Assuming the same variance r_x for $r(k)$ and $s(k)$ clearly corresponds to uniform distribution of the random phase shifts in $[-\pi,\pi]$. In the case of only small phase shifts around h, it would be preferable to reduce the variance of $s(k)$ accordingly. Minor changes would then be required from the equations presented here.

In conformity with BG restoration [1]-[3], the adopted detection/estimation strategy lies on marginal MAP (MMAP) detection of $\mathbf{q}$ and on MAP estimation of $\mathbf{x}$:

$$\hat{\mathbf{q}} \triangleq \arg\max P(\mathbf{q} \mid \mathbf{z}), \quad (4)$$

$$\hat{\mathbf{x}} \triangleq \arg\max p(\mathbf{x} \mid \hat{\mathbf{q}}, \mathbf{z}). \quad (5)$$

When $\mathbf{q}$ is known, $p(\mathbf{x} \mid \mathbf{q}, \mathbf{z})$ is Gaussian due to the linearity of the I/O model and to normal assumption on $\mathbf{x} \mid \mathbf{q}$. The estimate $\hat{\mathbf{x}}$ is easily obtained through the classical linear-Gaussian formulas :

$$\hat{\mathbf{x}} = \Pi H' B^{-1}\mathbf{z} \text{ with } B = H\Pi H' + \Gamma_n \quad (6)$$

where Π denotes the *a priori* covariance of $\mathbf{x} \mid \mathbf{q}$. From the definition of the DBG-process :

$$\Pi = r_x \begin{bmatrix} Q & 0 \\ 0 & Q \end{bmatrix} \text{ where } Q = \mathrm{Diag}(\mathbf{q}). \quad (7)$$

The most difficult task remains the detection step *i.e.* the maximization of $P(\mathbf{q} \mid \mathbf{z}) \propto P(\mathbf{z} \mid \mathbf{q})P(\mathbf{q})$ with respect to $\mathbf{q}$. Equivalently, since B is the covariance matrix of $\mathbf{z} \mid \mathbf{q}$, the detection criterion may be expressed in terms of B:

$$L_M(\mathbf{q}) = -\mathbf{z}'B^{-1}\mathbf{z} - \ln|B| - 2N_e \ln(1/\lambda - 1) \quad (8)$$

where N_e is the number of non-zero samples in $\mathbf{q}$.

3 IMPLEMENTED ALGORITHM. COLORED NOISE EXTENSION

3.1 Derivation of the algorithm

Here, we generalize the iterative SMLR-type algorithm introduced in [3] to DBG restoration, maintaining the same simple structure : given any initial $\mathbf{q}_0$ sequence, we explore a set of *neighbouring* sequences $\mathbf{q}_k$, $k = 1..N$, each of which differing from $\mathbf{q}_0$ only at site k. Then the one with the best MMAP criterion value is selected as the next initial value. This only guaranties convergence to a local optimum but it proves to be satisfactory in many practical cases.

Let $\mathbf{v}_k$ be the N-vector whose coordinates are 0 except for the kth one which is equal to 1, and V_k the $(2N \times 2)$-matrix defined by:

$$V_k = \begin{bmatrix} \mathbf{v}_k & 0 \\ 0 & \mathbf{v}_k \end{bmatrix} \quad (9)$$

Following [3] we introduce the auxiliary quantities:

$$A \triangleq H'B^{-1}H,\ \mathbf{w} \triangleq H'B^{-1}\mathbf{z} \quad (10)$$

$$\text{and } R_k \triangleq \epsilon_k r_x^{-1} I_2 + V_k' A_0 V_k \quad (11)$$

where ϵ_k takes the value 1 (resp. -1) when a 1 is added to (resp. removed from) sequence $\mathbf{q}_0$. Let us seek a relationship between $L_M(\mathbf{q}_k)$ and $L_M(\mathbf{q}_0)$. From (7) and (6) we derive

$$\Pi_k = \Pi_0 + \epsilon_k r_x V_k V_k' \quad (12)$$

$$B_k = B_0 + \epsilon_k r_x H V_k V_k' H'. \quad (13)$$

Application of the inversion lemma to B_k yields:

$$B_k^{-1} = B_0^{-1} - B_0^{-1} H V_k R_k^{-1} V_k' H' B_0^{-1} \quad (14)$$

From (14)(10) we update A and $\mathbf{w}$:

$$A_k = A_0 - A_0 V_k R_k^{-1} V_k' A_0 \quad (15)$$

$$\mathbf{w}_k = \mathbf{w}_0 - A_0 V_k R_k^{-1} V_k' \mathbf{w}_0 \quad (16)$$

and from (11)(13) we derive (see [5], Appendix A)

$$|B_k| = |B_0|\, r_x^2\, |R_k| \quad (17)$$

Using (8)(10)(14)(17) we update L_M:

$$L_M(\mathbf{q}_k) = L_M(\mathbf{q}_0) + \mathbf{w}_0' V_k R_k^{-1} V_k' \mathbf{w}_0 + \delta\psi \quad (18)$$

$$\delta\psi \triangleq -\ln(|R_k|\, r_x^2) - 2\epsilon_k \ln(1/\lambda - 1)$$

Using the previous equations we derive the algorithm designed to (suboptimally) maximize L_M:

1. **initialization**
   $\mathbf{q}_0 = \mathbf{0}$, specify z, H, Γ_n, r_x, λ
   compute $A_0 = H'\Gamma_n^{-1}H$ (see 3.2)
   compute $\mathbf{w}_0 = H'\Gamma_n^{-1}\mathbf{z}$ (see 3.2)
   compute $L_M(\mathbf{q}_0)$
2. **iteration**
   for $k = 1 \cdot\cdot N$: compute $L_M(\mathbf{q}_k)$ using (18)
   select $\hat{\mathbf{q}} = \arg\max L_M(\mathbf{q}_k)$
3. **convergence test**
   if $L_M(\hat{\mathbf{q}}) \leq L_M(\mathbf{q}_0)$ **then**
   compute $\hat{\mathbf{x}} = \Pi\mathbf{w}_0$
   stop
   else
   update $\mathbf{q}_0 = \hat{\mathbf{q}}$
   update $L_M(\mathbf{q}_0) = L_M(\hat{\mathbf{q}})$ using (8)
   update A_0 using (15)
   update $\mathbf{w}_0$ using (16)
   back to 2

The most costly steps of this algorithm are the initialization step and the update of A, the latter being of order $O(4N^2)$, whereas expressions like A_0V_k or $V_k'\mathbf{w}_0$ do actually involve no arithmetic operation. Uncautious computation of $A_0 = H'\Gamma_n^{-1}H$ may lead to an initialization step of order $O(N^3)$ which would geopardize the efficiency of the overall procedure. Initialization issues are treated in the next subsection. Provided the initialization was handled properly, the sequences to be estimated are sparse so that only few iterations are needed before convergence. The manipulation and storage of the $(2N \times 2N)$-matrix A remains the main computational burden.

3.2 Colored noise and initialization

A particularity of the algorithm presented above is that noise and I/O model specifications appear only in the initialization step. From the algorithmic point of view, this is a very positive feature since the implementation of colored noise extension merely requires a modification of the initial step. In principle the algorithm would run given any specification of noise covariance Γ_n or I/O model H, provided we pay the price for it : an initialization of order $O(N^3)$. In the following, we show that in the case of the retained I/O model and of a Gaussian AR model for the noise the cost is lower than $O(N^2)$. This means that we impose a structure on the relevant matrices in order to spare computation time. The exact structure of the matrix H depends on the kind of windowing assumptions on the input. We will here treat the case of pre-windowing but similar results are available for different choices. Then the matrices H_1 and H_2 are square lower-triangular Toeplitz (LTT) matrices. The initial values of A and $\mathbf{w}$ take the following form:

$$A_0 = \begin{bmatrix} H_1'\Gamma_n^{-1}H_1 & H_1'\Gamma_n^{-1}H_2 \\ H_2'\Gamma_n^{-1}H_1 & H_2'\Gamma_n^{-1}H_2 \end{bmatrix} \mathbf{w}_0 = \begin{bmatrix} H_1'\Gamma_n^{-1}\mathbf{z} \\ H_2'\Gamma_n^{-1}\mathbf{z} \end{bmatrix}.$$

We assume now that n is a Gaussian AR of order p. By the Gohberg-Semencul formula [6], Γ_n^{-1} admits the factorization $\Gamma_n^{-1} = L'L - P'P$ where L and P are both LTT matrices. Moreover, their coefficients have a simple expression in terms of the AR parameters and variance of generating noise. As shown before, the initial step requires matrix products like:

$$H_i'\Gamma_n^{-1}H_j = (LH_i)'(LH_j) - (PH_i)'(PH_j)$$
$$H_i'\Gamma_n^{-1}\mathbf{z} = (LH_i)'L\mathbf{z} - (PH_i)'P\mathbf{z}.$$

The matrices (LH_j) and (PH_j) are LTT as the product of LTT matrices. It follows that computation of say $(LH_i)'(LH_j)$ only involves products between the first column of (LH_i) and (LH_j). Thus it requires $O((l+p)^2)$ multiplications if $i \neq j$ and half as much otherwise ($(l+1)$ is the size of the wavelet). It can be shown as well that the computation of $(LH_i)'L\mathbf{z}$ amounts $O(N(l+2p))$ multiplications. The other computations cost even less. Thus the overall cost of initialization remains under $O(N^2)$.

4 NUMERICAL RESULTS

Performance of BG and DBG methods are compared on both synthetic and real data. The first example is a modification of Mendel's one [1] (see Fig. 1). Practically, we assigned a random imaginary part to each reflector, corresponding to a uniformly distributed phase in $[-\pi/4, \pi/4]$. Secondly, we replaced the classical fourth order wavelet by its autocorrelation, because the unrealistic high frequency content of the former yields a pathological Hilbert transform. Incidentally, the deconvolution problem becomes more difficult because of high frequency attenuation. Then we added a Gaussian AR noise whose characteristics are borrowed from the real data example of Fig. 2. A standard SNR value of 10dB was chosen. BG and colored DBG results are shown on Fig. 1. Only few false alarms and non detections appear in the DBG result, which compares favorably to BG one, especially when phase shifts are large.

The second example was drawn from a real experiment in the area of CND. It consists of a set of normal incidence Ascans collected by a focused transducer on a ferritic steel block. The acoustic manifestation of holes drilled in the block can be seen on Fig. 2. The (saturated) frontwall and backwall echoes have been gated away. The wavelet used for restoration was obtained by stacking the backwall echoes. Here, due to the complexity of propagation, the classical model (convolution + white noise) appears too rough and the BG method fails to account for the impulsive nature of the reflection. In order to perform DBG restoration, noise AR parameters were separately identified on a trace without reflector. Accurate detection is demonstrated by the DBG results depicted on Fig 2.

5 CONCLUSION

In this paper we extended the well-known BG deconvolution to cope with phase shift nonstationnarities encountered in areas such as Geophysics and CND. We showed that a SMLR structure could be maintained at a moderate extra computationnal cost. Numerical experiments indicate an increased robustness compared to standard BG methods. This is a very positive feature as regards real data processing.

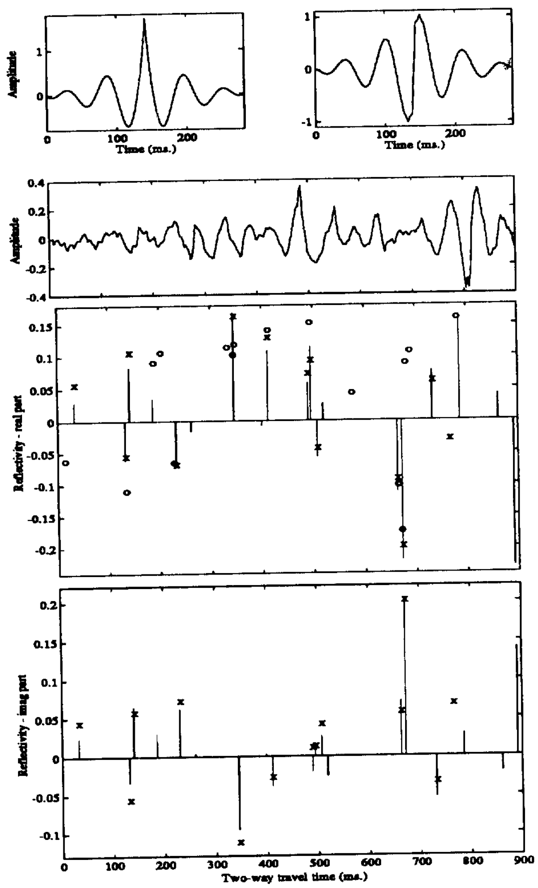

Fig. 1: Comparative deconvolution on the modified Mendel exemple. Top: the wavelet, its Hilbert transform and synthetic data. Middle: Mendel sequence (|), BG (o) and DBG (x) deconvolution. Bottom: Imaginary part of input sequence (|) and DBG (x) result.

6 REFERENCES

[1] J. Kormylo and J.M. Mendel, "Maximum likelihood detection and estimation of Bernoulli-Gaussian processes," *IEEE Trans. on IT*, **IT-28**, pp. 482–488, 1982.

[2] J. Goutsias and J.M. Mendel, "Maximum likelihood deconvolution : An optimization theory perspective," *Geophysics*, **51**, pp. 1206–1220, 1986.

[3] Y. Goussard, G. Demoment and J. Idier, "A new algorithm for iterative deconvolution of sparse spike trains," *Proc. Int. Conf. ASSP*, Albuquerque, New Mexico, pp. 1547–1550, 1990.

[4] S. Levy and D.W. Oldenburg, "Automatic phase correction of common-midpoint stacked data" *Geophysics*, **52**, pp. 51–59, 1987.

[5] J. Idier and Y. Goussard, "Multichannel seismic deconvolution" to appear in *IEEE Trans. on GE*.

[6] S.M. Kay, *Modern spectral estimation*, Prentice-Hall, 1988.

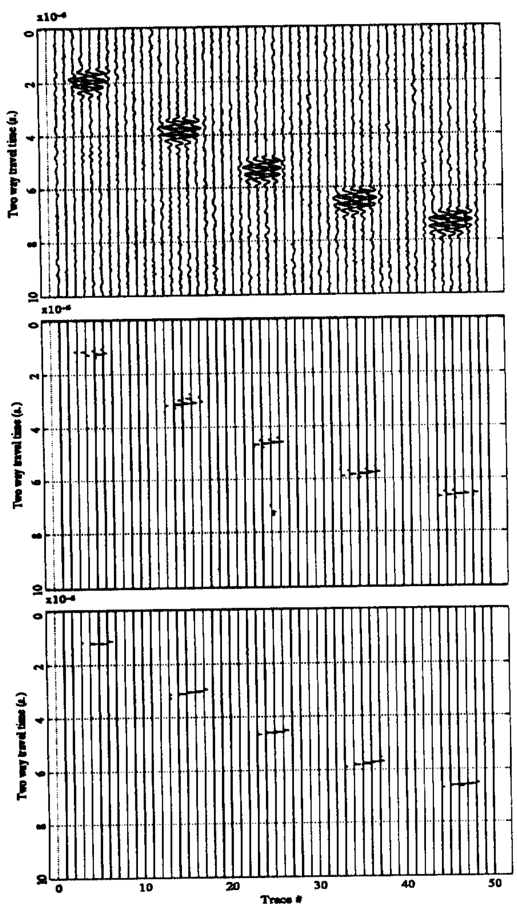

Fig. 2: Top : Normal incidence Bscan (frontwall and backwall echo removed). Middle : BG deconvolution. Bottom : DBG deconvolution.